Joint iterative migration of surface and borehole gravity gradiometry data

Muran Han, Le Wan, and Michael S. Zhdanov, University of Utah and Technoimaging*

Summary

Gravity and gravity gradiometry surveys have been widely used in mining and petroleum exploration. Interest in borehole gravity measurements has grown because they can help to detect deep targets. The best way to obtain a 3D density distribution is by the joint interpretation of surface and borehole gravity data which is a very challenging problem. The 3D inversion would be a choice for the quantitative interpretation of gravity and gravity gradiometry data. However, it is a complicated and time consuming procedure that is very dependent on the a priori model and constraints used. This paper demonstrates that joint iterative migration of surface and borehole gravity and gravity gradiometry data can effectively image subsurface density distribution.

Introduction

High quality gravity gradiometry data can be acquired from either airborne or marine platforms over very large areas for relatively low cost. However, the sensitivities of the gravity field and its gradients are inversely proportional to the square or cube of the distance, respectively. Making use of the borehole gravity measurement can significantly improve the inversion or migration results. The goal of this paper is to combine the surface and borehole gravity and gravity gradient data to obtain better migration images of the subsurface. The borehole gravity method was pioneered by Smith (1950) and then applied to problems of reservoir evaluation by McCulloh et al. (1968). Unlike the shallower-sensing density log, the borehole gravimeter is insensitive to wellbore conditions such as rugosity and the presence of casing. The advantages of measuring gravity gradients rather than the gravity field have also been recognized (e.g., Nekut, 1989). The borehole gravity log results have also been reported in many papers (for example, McCulloh et al., 1968; Rasmussen 1975; Jageler, 1976; LaFehr, 1983; Gournay et al., 1984; Popta et al., 1990; Alixant and Mann, 1995; Brady et al., 2006; Nind et al., 2007; MacQueen, 2007; and Krieger et al., 2009). The prototype borehole gravity gradiometers have since been developed (e.g., Golden et al., 2007).

Many researchers have tried to combine the borehole and the surface gravity data to improve the results of interpretation. For example, Cao (2013) inverted the surface and borehole seismic data jointly to overcome the narrower frequency bandwidth defects of the surface seismic data. Li and Oldenburg (2000) inverted the surface and borehole magnetic data jointly to better define the deeper target. Krahenbuhl and Li (2008) and Sun and Li (2010) published the results of the joint inversion of surface and borehole gravity data. Also, Rim and Li (2010) and Liu and Zhdanov (2011) conducted the research for a single borehole data imaging.

Migration of gravity fields is a fast imaging tool to locate a target using a transformation of the observed data into a 3D density image (Zhdanov, 2002). The results are the same as those of 3D inversion; however, the numerical implementation and physical interpretation are different. It has been used in the interpretation of practical gravity and gravity gradient data as a fast imaging tool (Zhdanov et al., 2011). The migration can be done iteratively and can be applied in the same way as inversion for the gravity and gravity gradiometry data (Wan and Zhdanov, 2013; Wan et al., 2016).

This paper demonstrates that the joint iterative migration of surface and borehole gravity gradiometry data can provide an improved representation of the subsurface density distribution and improve the imaging of a deep target.

Migration of surface gravity and gravity tensor fields and 3D density imaging

Let us assume that we have observed some component of the surface gravity field $\boldsymbol{g}_\alpha^S(\mathbf{r})$ and/or some surface gravity gradients $\boldsymbol{g}_{\alpha\beta}^S(\mathbf{r})$ over an observational surface S, located in the air or on the ground. The problem is to determine the 3D density distribution, $\rho(\mathbf{r}')$, under the ground.

Following Zhdanov (2002), the surface *migration gravity field*, $\boldsymbol{g}_\alpha^{Sm}(\mathbf{r})$, is introduced as a result of application of the adjoint gravity operator, $\boldsymbol{A}_\alpha^{S*}$, to the observed component of the surface gravity field $\boldsymbol{g}_\alpha^S$:

$$\boldsymbol{g}_\alpha^{Sm}(\mathbf{r}) = \boldsymbol{A}_\alpha^{S*}\boldsymbol{g}_\alpha^S, \tag{1}$$

where the adjoint operator $\boldsymbol{A}_\alpha^{S*}$ for the gravity problem (Zhdanov et al., 2011) is equal to:

$$\boldsymbol{A}_\alpha^{S*}(f) = \iint_S \frac{f(\mathbf{r})}{|\mathbf{r}'-\mathbf{r}|^3} K_\alpha(\mathbf{r}'-\mathbf{r})ds. \tag{2}$$

From the physical point of view, the migration field is obtained by moving the sources of the observed gravity field above the observational surface. Nevertheless, the migration field contains some remnant information about the original sources of the gravity anomaly. That is why it can be used in imaging the sources of the gravity field.

In a similar way, we can introduce a surface *migration gravity tensor field* $\boldsymbol{g}_{\alpha\beta}^{Sm}(\mathbf{r})$ and use the following notations for the components of this tensor field:

$$\boldsymbol{g}_{\alpha\beta}^{Sm}(\mathbf{r}) = \boldsymbol{A}_{\alpha\beta}^{S*}\boldsymbol{g}_{\alpha\beta}^{S}, \tag{3}$$

where the adjoint operators, $\boldsymbol{A}_{\alpha\beta}^{S*}$, applied to some function $f(\mathbf{r})$, are given by the formulas:

$$\boldsymbol{A}_{\alpha\beta}^{S*}(f) = \iint_S \frac{f(\mathbf{r})}{|\mathbf{r}'-\mathbf{r}|^3} K_{\alpha\beta}(\mathbf{r}'-\mathbf{r})ds. \tag{4}$$

We can find a distribution of the density of the gravity field sources, described by the following expression:

$$\rho_{\alpha}^{Sm}(\mathbf{r}) = k_{\alpha}^{S} w_{\alpha}^{S}(z) g_{\alpha}^{Sm}, \tag{5}$$

where unknown coefficient k_{α}^{S} can be determined by a linear line search (Zhdanov, 2002) according to the following:

$$k_{\alpha}^{S} = \frac{\left\|A_{\alpha}^{w*} g_{\alpha}^{S}\right\|_M^2}{\left\|A_{\alpha}^{w} A_{\alpha}^{w*} g_{\alpha}^{S}\right\|_D^2}, \tag{6}$$

$$A_{\alpha}^{w} = A_{\alpha}^{S} W_{\alpha}^{-1}, \tag{7}$$

and the linear weighting operator $W_m = W_\alpha$ is selected as a linear operator of multiplication of the density ρ by a function, w_α; equal to the square root of the integrated sensitivity of the complex intensity of the gravity field, S_α:

$$w_{\alpha}^{S} = \sqrt{S_{\alpha}^{S}} \tag{8}$$

In a similar way, we can introduce a migration density based on the gravity tensor migration:

$$\rho_{\alpha\beta}^{Sm}(\mathbf{r}) = k_{\alpha\beta}^{S}\left(w_{\alpha\beta}^{S}\right)^{-2}\boldsymbol{g}_{\alpha\beta}^{Sm}(\mathbf{r}), \tag{9}$$

where:

$$k_{\alpha\beta}^{S} = \frac{\left\|A_{\alpha\beta}^{w*} g_{\alpha\beta}^{S}\right\|_M^2}{\left\|A_{\alpha\beta}^{w} A_{\alpha\beta}^{w*} g_{\alpha\beta}^{S}\right\|_D^2}, \tag{10}$$

Functions $w_{\alpha\beta}^{S}$ are equal to the square root of the integrated sensitivity of the gravity tensor fields, $S_{\alpha\beta}^{S}$, respectively:

$$w_{\alpha\beta}^{S} = \sqrt{S_{\alpha\beta}^{S}} \tag{11}$$

Migration of borehole gravity and gravity tensor fields and 3D density imaging

Let us assume that we have observed some component of the borehole gravity field $\boldsymbol{g}_{\alpha}^{B}(\mathbf{r})$ and/or some borehole gravity gradients $\boldsymbol{g}_{\alpha\beta}^{B}(\mathbf{r})$ along an observational line L, associated with a given borehole. The problem is to determine the 3D density distribution, $\rho(\mathbf{r}')$, around the borehole. Following Zhdanov (2002, 2011), the borehole *migration gravity field*, $\boldsymbol{g}_{\alpha}^{Bm}(\mathbf{r})$, is introduced as a result of application of the adjoint gravity operator, $\boldsymbol{A}_{\alpha}^{B*}$ to the observed gravity field:

$$\boldsymbol{g}_{\alpha}^{Bm}(\mathbf{r}) = \boldsymbol{A}_{\alpha}^{B*}\boldsymbol{g}_{\alpha}^{B}, \tag{12}$$

where the adjoint operator $\boldsymbol{A}_{\alpha}^{B*}$ for the borehole gravity problem is equal:

$$\boldsymbol{A}_{\alpha}^{B*}(f) = \int_L \frac{f(\mathbf{r})}{|\mathbf{r}'-\mathbf{r}|^3} K_{\alpha}(\mathbf{r}'-\mathbf{r})dl, \tag{13}$$

In a similar way, we can introduce a migration field $\boldsymbol{g}_{\alpha\beta}^{Bm}(\mathbf{r})$ of the borehole gravity tensor components observed along a borehole L, and use the following notations for the components of this tensor field:

$$\boldsymbol{g}_{\alpha\beta}^{Bm}(\mathbf{r}) = \boldsymbol{A}_{\alpha\beta}^{B*}\boldsymbol{g}_{\alpha\beta}^{B}, \tag{14}$$

where the corresponding adjoint operators, $\boldsymbol{A}_{\alpha\beta}^{B*}$, applied to some function $f(\mathbf{r})$, are given by:

$$\boldsymbol{A}_{\alpha\beta}^{B*}(f) = \int_L \frac{f(\mathbf{r})}{|\mathbf{r}'-\mathbf{r}|^3} K_{\alpha\beta}(\mathbf{r}'-\mathbf{r})dl. \tag{15}$$

Using the same principles as we discussed above for migration of the surface data, one can calculate the density distribution by migration of the borehole data.

Joint migration

Our goal is to jointly migrate the surface and borehole gravity fields to make a clear image of a deep target. We consider a joint migration of the multiple components of the surface and borehole gravity and gravity tensor fields according to the following formula:

$$\rho^m(\mathbf{r}) = c_{\alpha}^{S}\rho_{\alpha}^{S}(\mathbf{r}) + \sum c_{\alpha\beta}^{S}\rho_{\alpha\beta}^{S}(\mathbf{r}) + c_{\alpha}^{B}\rho_{\alpha}^{B}(\mathbf{r}) + \sum c_{\alpha\beta}^{B}\rho_{\alpha\beta}^{B}(\mathbf{r}), \tag{16}$$

where c_{α}^{S}, $c_{\alpha\beta}^{S}$, c_{α}^{B}, and $c_{\alpha\beta}^{B}$ can be treated as the weights of the corresponding migration fields in the density model, which can be empirically determined from the results of the model studies.

We use the following expressions for joint migration, which provides an averaging for both the surface and borehole data:

$$\rho^m(\mathbf{r}) = c_1\frac{\rho_{\alpha}^{S}(\mathbf{r}) + \sum\rho_{\alpha\beta}^{S}(\mathbf{r})}{N_S+1} + c_2\frac{\rho_{\alpha}^{B}(\mathbf{r}) + \sum\rho_{\alpha\beta}^{B}(\mathbf{r})}{N_B+1}, \tag{17}$$

if the gravity field is used in the migration, or:

$$\rho^m(\mathbf{r}) = c_1\left(\sum\rho_{\alpha\beta}^{S}(\mathbf{r})\right)/N_S + c_2\left(\sum\rho_{\alpha\beta}^{B}(\mathbf{r})\right)/N_B. \tag{18}$$

if the gravity field is not used. In the last formulas, N_S is the number of the surface gravity gradient components, the N_B is the number of borehole gravity gradient components, and c_1 = 0.5 and c_2 = 0.5.

10.1190/segam2018-2996358.1

Iterative migration

Equation (17) or (18) produces a migration image of density distribution in the lower half-space. A better quality migration image can be produced by repeating the migration process iteratively (Wan and Zhdanov, 2013). We begin with the migration of the observed gravity and/or gravity tensor field data and get the density distribution. In order to check the accuracy of our migration imaging, we apply the forward modeling and compute a residual between the observed and predicted data for the given density model.

$$\boldsymbol{r}_1 = \boldsymbol{g}^{pre} - \boldsymbol{g}^{obs} \tag{19}$$

where $\boldsymbol{g}^{obs}$ is the observed gravity or gravity gradient component, $\boldsymbol{g}^{pre}$ is the predicted gravity or gravity gradient component. If the residual is smaller than the prescribed accuracy level, we use the migration image as a final density model. In the case where the residual is not small enough, we migrate the residual field and produce the density, $\delta\rho_1^m$, to the original density model using the same analysis, which we have applied for the original migration.

A general scheme of the iterative migration can be described by the following formula:

$$\rho_{n+1}^m = \rho_n^m - \delta\rho_n^m \tag{20}$$

The iterative migration is terminated when the residual field becomes smaller than the required accuracy level of the data fitting.

The iterative migration can be combined with regularization method. This also allows to apply the smooth or focusing stabilizers to produce a more focused image of the target (Wan and Zhdanov, 2013).

Model study

In this section we present an example of 3D joint migration for surface and borehole gravity gradient field data. We consider a model, which contains two reservoirs, the size of 1000 m x 1000 m x 200 m (L x W x H), one above the other. The upper reservoir is located at a depth of 0.9 *km* below the surface, and the lower reservoir is located at 1.9 *km* below the surface (see Figure 1).

The surface gravity sensors are distributed within the range of 6 km in the x direction and 5.6 km in the y direction with 100 m separation in the x and y directions. A vertical borehole is located at the poring with the coordinates of x = 3000 m and y = 2200 m. The interval of observation in the borehole is 5 m in the z direction. The observed data contained 5% random noise.

Figure 2 shows as an example the results of iterative migration of the surface g_{zz} component only at the cross section of x = 3000 *m*. The blue line shows the observed data and the red line represents the predicted data at the surface (top panel). One can see that the migration density image shows one target only, the lower reservoir cannot be seen at all from the surface data, even though the data fitting is very good, as shown in the top panel of the Figure 2.

Now, we consider the migration of the borehole data. Figure 3 presents the results of iterative migration of the borehole g_{zz} data. The blue line shows the observed data and the red line represents the predicted data in the borehole (side panel). The migration density image shows that it is possible to resolve two reservoirs from the borehole data. However, the artifacts on the opposite side from the borehole complicate the image.

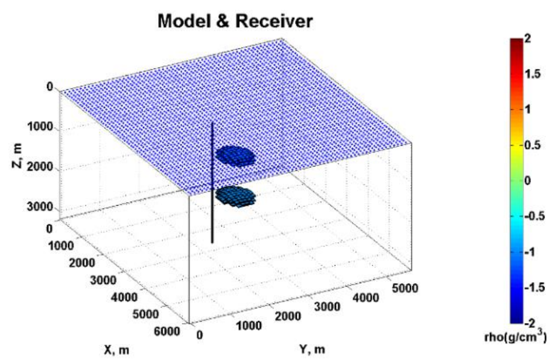

Figure 1: Model of two HC reservoirs. The blue dots show the observation stations at the surface. The vertical black dots denote the position of the borehole.

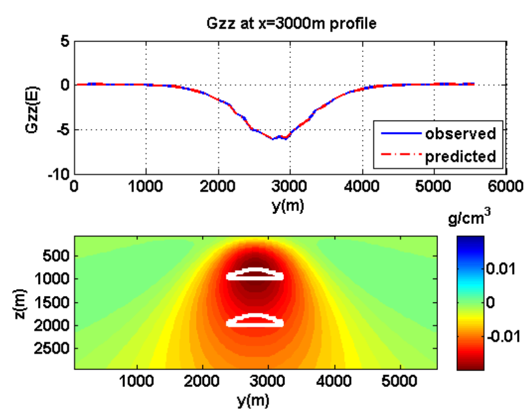

Figure 2: The result of iterative migration of surface g_{zz} component only at the cross section of x = 3000 *m* (bottom panel). The blue line shows the observed data and red line shows the predicted data at the surface (top panel).

10.1190/segam2018-2996358.1

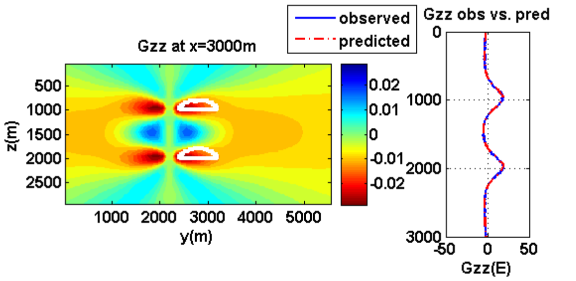

Figure 3: The result of iterative migration of surface g_{zz} component only at the cross section of x = 3000 m (left panel). The blue line shows the observed data and red line shows the predicted data at the surface (right panel).

In the next step of our numerical study, we consider a joint migration of the surface and borehole gravity data. Figure 4 shows the result of the iterative migration of the surface g_{yz} component and borehole g_{yz} component jointly. The migration density image reconstructs two reservoirs clearly enough in this figure.

Finally, Figure 5 presents the results of joint iterative migration of the surface and borehole $g_{zz} + g_{yz}$ data. The migration transformation in this case provides a clean image of the two targets without any artifacts.

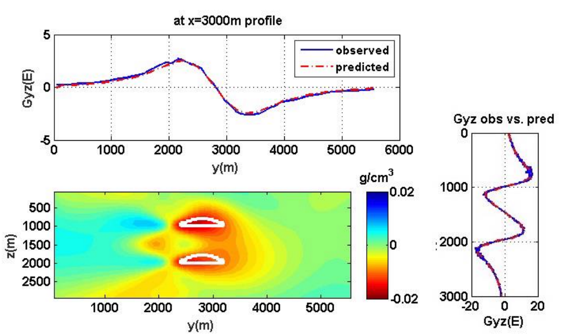

Figure 4: The result of joint iterative migration of surface and borehole g_{yz} component only at the cross section of x = 3000 m (bottom left panel). The blue line shows the observed data and red line shows the predicted data at the surface (top panel) and in the borehole (right panel).

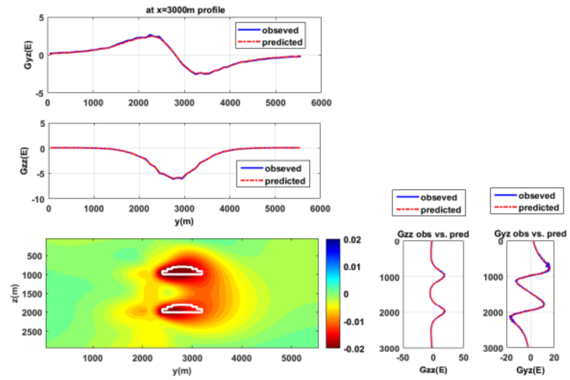

Figure 5: The result of joint iterative migration of surface and borehole $g_{zz} + g_{yz}$ data at the cross section of x = 3000 m (bottom left panel). The blue line shows the observed data and red line shows the predicted data at the surface (top panel) and in the borehole (right panels).

Conclusions

We have developed a novel approach to interpretation of the gravity gradiometry data by considering the joint iterative migration of the data observed both on the surface and in the borehole. The numerical modeling study has demonstrated that this approach provides an efficient tool for rapid imaging of gravity gradiometry data. Our results also show that by migrating the borehole data jointly with the surface data, we obtain a vertical resolution of the inversion, which would be otherwise impossible to achieve with surface observation only. Thus, this research shows the importance of developing gravity gradiometry systems capable of measuring the gravity tensor field in the borehole.

Acknowledgments

The authors acknowledge the support of the University of Utah Consortium for Electromagnetic Modeling and Inversion (CEMI).

The authors also acknowledge TechnoImaging for support of this research.

10.1190/segam2018-2996358.1

REFERENCES

Alixant, J.-L., and E. Mann, 1995, In-situ residual oil saturation to gas from time-lapse borehole gravity: Presented at the SPE Annual Technical Conference and Exhibition, https://doi.org/10.2118/30609-MS.

Brady, J. L., J. L. Hare, J. F. Ferguson, J. E. Seibert, F. J. Klopping, T. Chen, and T. Niebauer, 2006, Results of the world's first 4D microgravity surveillance of a waterflood—Prudhoe Bay, Alaska: Presented at SPE Annual Technical Conference and Exhibition, https://doi.org/10.2118/101762-MS.

Cao, D., 2013, Impedance joint inversion of surface and borehole seismic data, AAPG Search and Discovery Article #90187 © CSPG/CSEG/CWLS GeoConvention 2013, Integration: Geoscience Engineering Partnership.

Golden, H., W. McRae, and A. Veryaskin, 2007, Description of and results from a novel borehole gravity gradiometer: Presented at ASEG 19th Geophysical Conference and Exhibition, https://doi.org/10.1071/ASEG2007ab047.

Gournay, L. S., and W. D. Lyle 1984, Determination of hydrocarbon saturation and porosity using a combination Borehole Gravimeter (BHGM) and deep investigating electric log: Presented at the SPWLA 25th Annual Logging Symposium.

Jageler, A. H. 1976, Improved hydrocarbon reservoir evaluation through use of borehole-gravimeter data: Journal of Petroleum Technology, **28**, 709–718, https://doi.org/10.2118/5511-PA.

Krahenbuhl, R., and Y. Li, 2008, Joint inversion of surface and borehole 4D gravity data for continuous characterization of fluid contact movement: 78th Annual International Meeting, SEG, Expanded Abstracts, 726–729, https://doi.org/10.1190/1.3063750.

Krieger, M., P. Smilde, and O. Geisler, 2009, Completing the image with borehole gravity gradients: 79th Annual International Meeting, SEG, Expanded Abstracts, 923–926, https://doi.org/10.1190/1.3255902.

LaFehr, T. R., 1983, Rock density from borehole gravity surveys: Geophysics, **48**, 341–356, https://doi.org/10.1190/1.1441472.

Li, Y., and D. W. Oldenburg, 2000, Joint inversion of surface and three-component borehole magnetic data: Geophysics, **65**, 540–552, https://doi.org/10.1190/1.1444749.

Liu, X., and M. Zhdanov, 2011, 3D imaging of gravity gradiometry data from a single borehole using potential field migration: SEG San Antonio 2011 Annual Meeting.

MacQueen, J. D. 2007, High-resolution density from borehole gravity data: 87th Annual International Meeting, SEG, Expanded Abstracts, 741–744, https://doi.org/10.1190/1.2792520.

McCulloh, T. H., G. R. Kandle, and J. E. Schoellhamer, 1968, Application of gravity measurements in wells to problems of reservoir evaluation: Society of Professional Well Log Analysts 9th Annual Logging Symposium Transactions, 1–29.

Nekut, A. G., 1989, Borehole gravity gradiometry: Geophysics, **54**, 225–234, https://doi.org/10.1190/1.1442646.

Nind, C., H. O. Seigel, M. Chouteau, and B. Giroux, 2007, Development of a borehole gravimeter for mining applications: First Break, **25**, 71–77.

Popta, J. V., J. M. T. Heywood, S. J. Adams, and D. R. Bostock, 1990, Use of borehole gravimetry for reservoir characterisation and fluid saturation monitoring: Proceedings of Europec 90, 151–160, https://doi.org/10.2118/20896-MS.

Rasmussen, N. F. 1975, Successful use of the borehole gravity meter in Northern Michigan: The Log Analyst, 3–10.

Rim, H., and Y. Li, 2010, Single-borehole imaging using gravity gradiometer data: 80th Annual International Meeting, SEG, Expanded Abstracts, 1137–1140, https://doi.org/10.1190/1.3513045.

Smith, N. J., 1950, The case for gravity data from boreholes: Geophysics, **15**, 605–636, https://doi.org/10.1190/1.1437623.

Sun, J., and Y. Li, 2010, Inversion of surface and borehole gravity with thresholding and density constraints: SEG Denver 2010 Annual Meeting.

Wan, L., and M. Zhdanov, 2013, Iterative migration of gravity and gravity gradiometry data: SEG Houston 2013 Annual Meeting, https://doi.org/10.1190/segam2013-1036.1.

Wan, L., M. Han, and M. Zhdanov, 2016, Joint iterative migration of surface and borehole of gravity and gravity gradiometry data: SEG Dallas 2016 Annual Meeting.

Zhdanov, M. S., 2002, Geophysical inverse theory and regularization problems: Elsevier.

Zhdanov, M. S., X. Liu, L. Wan, and G. Wilson, 2011, 3D potential field migration for rapid imaging of gravity gradiometry data: Proceedings of Annual Meeting of the Consortium for Electromagnetic Modeling and Inversion.

10.1190/segam2018-2996358.1